Journal of Materials Chemistry A

Accepted Manuscript

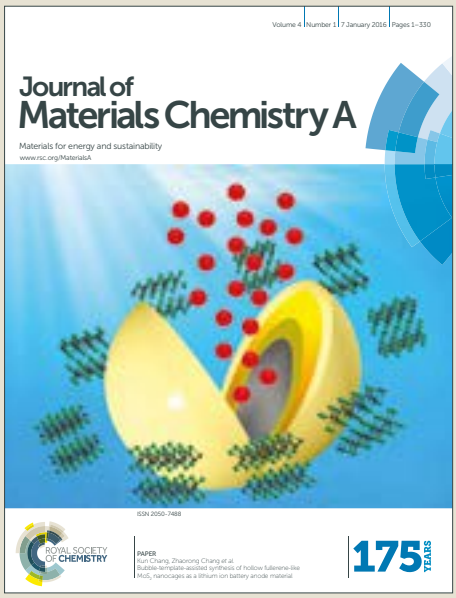

ROYAL SOCIETY OF CHEMISTRY

rsc.li/materials-a

View Article Online
DOI: 10.1039/C7TA06199D

Journal Name

COMMUNICATION

Fine-tuning of the confined space in microporous metal-organic frameworks for efficient mercury removal

Received 00th January 20xx,
Accepted 00th January 20xx

DOI: 10.1039/x0xx00000x

www.rsc.org/

Marta Mon,[a] Xiaoni Qu,[a,b] Jesús Ferrando-Soria,*[a] Isaac Pellicer-Carreño,[c] Antonio Sepúlveda-Escribano,[c] Enrique V. Ramos-Fernandez,[c] Johannes C. Jansen,[d] Donatella Armentano*[e] and Emilio Pardo*[a]

Abstract: Offsetting the impact of human activities on the biogeochemical cycle of mercury has become a compelling demand towards a sustainable planet. Here, we report our investigations to develop a water-stable and eco-friendly metal-organic framework, of formula $\{Cu^{II}_4[(S,S)\text{-methox}]_2\} \cdot 5H_2O$ (1), where methox is bis[(*S*)-methionine]oxalyl diamide, featuring narrow functional channels decorated with thioalkyl chains able to capture $HgCl_2$ from aqueous media in an efficient, selective and rapid manner. The conscious design effort in terms of size, shape and reactivity of the channels, yields an extremely efficient immobilization of the $HgCl_2$ guest species in a very stable conformation, reminiscent of the enzyme mercury reductase. Thus, 1 enables highly efficient removal of toxic $HgCl_2$ from aqueous media, reducing the $[Hg^{2+}]$ concentration from the dangerous 10 ppm to acceptable limits for drinking water, below 2 ppb. The unusual combination in 1 of a low-cost straightforward synthesis and high stability in environmental conditions, synergically connected to the efficient and rapid removal of poisonous mercury ions, places 1 among the most attractive adsorbents reported for the purification of contaminated water.

Metal-organic frameworks (MOFs)[1–5] have been in the spotlight in the last years given their wide varied functional properties.[6] Among them, stand out the selective capture and/or separation of gases[7] and small molecules[8] with relevance from an industrial and ecological points of view. The reason behind this high performance obeys to its exclusive combination of a fascinating host-guest chemistry[9–16] and high crystallinity, which confer MOFs with an unparalleled synthetic versatility underpinned by X-Ray Crystallography. This has allowed to improve their capture/separation properties by chemically engineering MOFs channels with the appropriate size, shape and reactivity,[17] or by post-synthetic modification,[18,19] So far, this enormous synthetic potential has already resulted in numerous examples of MOFs separating different gases of importance from both industrial and environmental viewpoints.[20–22] Conversely, molecular recognition with MOFs has been barely explored. Some promising results,[23,24] have shown the potential of MOFs on this area, but enormous opportunities in the encapsulation and separation of more complex molecular systems are yet waiting to be discovered.[1]

One of the greatest challenges the world faces today is the increasing heavy metal pollution caused by industrial activities and/or accidental discharges. In particular, highly toxic mercury derivatives are widespread in the environment,[25–28] including air, water and soil,[29,30] with the consequent threat to public health. Therefore, there is an urgent need for novel efficient methods to capture mercury, selectively.[31–37] MOFs are showing themselves recently as very attractive materials in this area.[38–44]

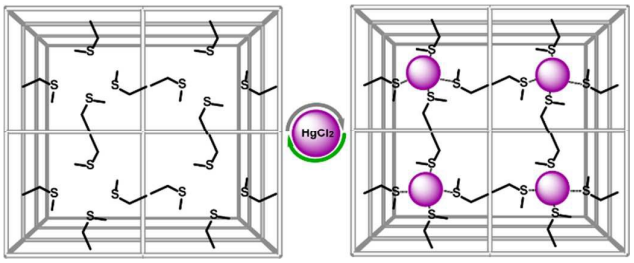

Scheme 1. Schematic representation of the capture of $HgCl_2$ (represented as purple spheres) from water by the thioether decorated porous network of **1**.

*Bio*inspired MOFs, in which the linker is evocative of the bio-world, can take advantage from both their environmentally-friendly designs and the intrinsic capabilities of biomolecules to drive molecular recognition processes owing to the presence of several accessible metal binding sites and their intrinsic ability to self-organize in highly ordered

[a] Departamento de Química Inorgánica, Instituto de Ciencia Molecular (ICMOL), Universidad de Valencia, 46980 Paterna, Valencia, Spain.
[b] College of Chemistry and Materials Science, Northwest University, Xi'an 710069, China.
[c] Laboratorio de Materiales Avanzados, Departamento de Química Inorgánica-Instituto Universitario de Materiales, Universidad de Alicante, Alicante, Spain.
[d] Institute on Membrane Technology, ITM-CNR, Via P. Bucci 17/C, 87036 Rende, Italy.
[e] Dipartimento di Chimica e Tecnologie Chimiche, Università della Calabria, 87036, Rende, Italy.

† Electronic Supplementary Information (ESI) available: Preparation and physical characterization data. Crystallographic refinement details. Additional Figs. S1-13 and Tables S1-S4. CCDC 1558088-1558090. See DOI: 10.1039/x0xx00000x

View Article Online
DOI: 10.1039/C7TA06199D

structures through hydrogen bonding, π-stacking or coordination-driven self-assembly interactions. This enables the design and synthesis of *bio*MOFs with addressable and highly task-specific functionalities.

In this work we have synthesised a new water-stable microporous MOF, showing very narrow square functional channels, which are decorated with thioether groups (Scheme 1 and Fig. 1). We report the synthesis and characterization of this novel three-dimensional *bio*MOF,[45,46] prepared from an oxamidato-based ligand[42,47,48] derived from the natural amino acid methionine, of formula $\{Cu^{II}_4[(S,S)\text{-methox}]_2\}\cdot 5H_2O$ (**1**) featuring very narrow square functional channels (diameter *ca.* 0.4 nm). The concomitant presence of both thioether groups pointing towards the centre of the channels and the confined state provided by a narrow pore size endows **1** with a suited recognition site towards soft metal ions, should allow the formation of very stable species. Based on these factors, we set out to evaluate the efficiency of this material in the selective removal of $HgCl_2$ from contaminated waters (Scheme S1b).

Compound **1** was synthesized, in a multigram scale, as reported in the Experimental section (ESI†). Green hexagonal prisms of **1**, suitable for X-ray diffraction, were successfully synthesised by means of a slow diffusion technique (see experimental section in the ESI†). Thereafter, in order to determine the maximum $HgCl_2$ uptake capacity, crystals of **1** were suspended in a saturated solution of $HgCl_2$ in water/methanol (1:1). The capture process was monitored by measuring the $HgCl_2$ increase within the MOF at specific time intervals through Inductively Coupled Plasma-Mass Spectrometry (ICP-MS) and Scanning Electron Microscopy with Energy Dispersive X-ray spectroscopy (SEM/EDX). Thus, the kinetic profile of the adsorption process (Fig. S1 and Table S2) shows a very particular two-regime kinetics, involving first an extremely fast increase of the $HgCl_2$ loading in **1** (which is achieved in around 15 min.). This process gives a novel hybrid material, which could be isolated and identified as $(HgCl_2)_{0.5}@\{Cu^{II}_4[(S,S)\text{-methox}]_2\}\cdot 3H_2O$ (**0.5HgCl$_2$@1**). Subsequently, a much slower adsorption process that is only completed after two weeks yields the compound $HgCl_2@\{Cu^{II}_4[(S,S)\text{-methox}]_2\}\cdot 2H_2O$ (**HgCl$_2$@1**). The chemical identity of the two adsorbates **0.5HgCl$_2$@1** and **HgCl$_2$@1** were further confirmed by elemental (C, H, N, S) and Thermogravimetric (TGA) analyses, together with X-ray diffraction (XRD) techniques (see ESI†).

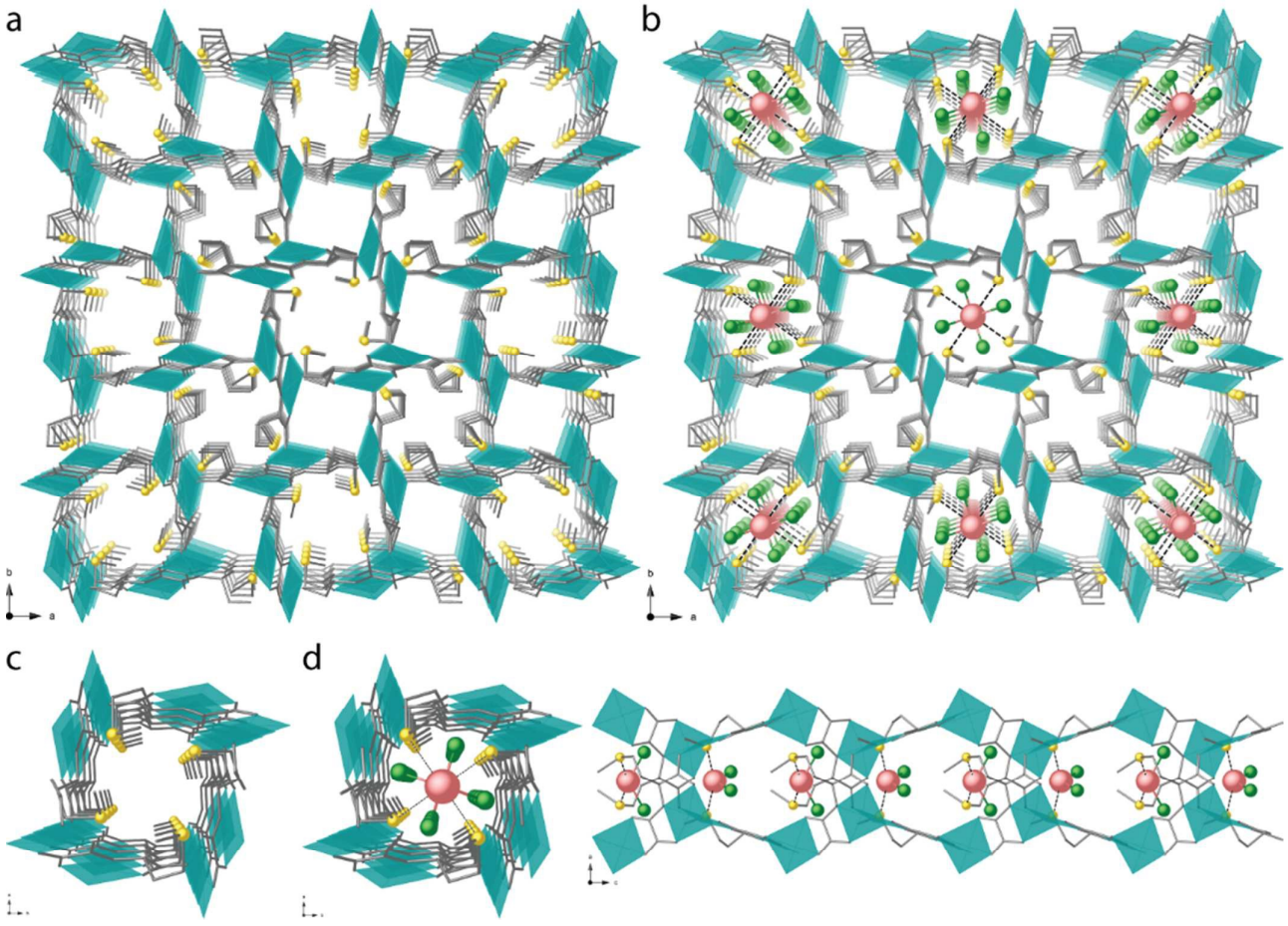

Fig. 1. Perspective views along the crystallographic *c* axis of the porous structure of **1** (**a**) and **0.5HgCl$_2$@1** (**b**). **c**. Detailed view of one single channel of **1** along the *c* axis. **d**. Side (left) and lateral (right) views of one channel of **0.5HgCl$_2$@1** (**d**) along *c* axis. Copper atoms and ligands (except S atoms) forming the network are represented by cyan polyhedra and grey sticks, respectively. Mercury, chloride and sulphur atoms are depicted as purple, green and gold spheres. Free water solvent molecules are omitted for clarity.

View Article Online
DOI: 10.1039/C7TA06199D

Journal Name

COMMUNICATION

The crystal structures of **1**, and of adsorbates **0.5HgCl$_2$@1** and **HgCl$_2$@1** could be determined by single-crystal X-ray diffraction (see ESI† for structural details and Figs. 1 and S2-S9) evidencing that the 3D network of the hosting matrix **1** remained crystalline during the inclusion process. They crystallize in the $P4_2$ space group of the tetragonal system and consist of a chiral 3D pillared square grid where [Cu^{II}_2(*S,S*)-methox] moieties are located on the vertices of the edges. The robust uni-nodal three-connected **srs** nets[49,50] with point symbol of (10^3) (Fig. S9) are built up from *trans* oxamidato-bridged dicopper(II) units, {Cu^{II}_2[(S,S)-methox]} (Fig. S2a), assembled each other through the carboxylate groups (Figs. S2b and S2c).

They feature three types of pores, different in size and shape, propagating along the *c* axis (Figs. 1, S3, S4 and S8) and enfolding up to 21% of the total lattice volume: Regularly spaced, hydrophilic square sized pores (virtual diameter of *ca* 0.32 nm) and two kinds of hydrophobic square pores of medium and larger size (virtual diameters of *ca.* 0.34 and 0.40 nm, respectively) (Figs 1a and S8b). The pore types result from the different disposition of the ethylenethiomethyl chains, pointing outwards or inwards of the voids. The chain conformations further affect the resulting host-guest chemistry. The crystal structures of the two adsorbates clearly evidence the presence of $HgCl_2$ guest molecules hosted in bigger hydrophobic square pores of **1**, clenched by the thioether chains of the methionine residues and confined into the channels *via* S···Hg interactions. In **0.5HgCl$_2$@1** and **HgCl$_2$@1**, only one of those hydrophobic channels is of an ideal size and shape to hold $HgCl_2$ molecules (Figs. 1b,c, S3-S5 and S8c,d). The mercury capture process is visually defined by the **0.5HgCl$_2$@1** and **HgCl$_2$@1** crystal structures, where only favoured pores and interstitial voids are filled by $HgCl_2$ molecules (Figs. 1 and S3).

The Hg^{2+} ions from both $HgCl_2$ molecules in **0.5HgCl$_2$@1** and **HgCl$_2$@1** (Figs. 1 and S3, respectively) and the chloride-bridged dinuclear $[Hg_2(\mu\text{-}Cl)Cl_2]^+$ entities (Fig. S7b), generated in **HgCl$_2$@1** (Figs. S3-S5) are tetracoordinated, being grasped by two sulphur atoms from the thioether groups belonging to the amino acid residues of the ligand (Figs. S6 and S7). They exhibit a highly distorted tetrahedral geometry, as a plausible consequence of the steric constrains forced by the host matrix (Figs. S6 and S7). The sulphur atom binds simultaneously to Hg(II) and Cu(II), in agreement with thioether S features found in literature.[51,52] The values of the Hg-S distances [2.86(1) Å (**0.5HgCl$_2$@1**), and 3.011(8) Å (**1HgCl$_2$@1**)] are in the range of those found in the literature.[53–55] Furthermore, even if longer, the Hg···S separation of dimeric species in **HgCl$_2$@1** [3.41(1) and 3.48(1) Å] (Fig. S7) suggests that a weak interaction may occur.

Despite the supposed flexibility and structural adaptability that the methionine residues offer,[42] no evident differences in the thioether chain conformations have been observed in **0.5HgCl$_2$@1** and **HgCl$_2$@1** adsorbates structures with respect to **1**. In all cases, thioether chains adopt a distended folding in such a way to confine ethylenethiomethyl arms in pores. Nonetheless, their conformations are stable either with ethylene chains entirely inside the channels, filling almost half of the volume of the medium pores, or confined in the interstitial voids within the walls of the net, pointing only the terminal -S-CH_3 thioether groups inside the pores. This behaviour guarantees **1** promising features as a high performing MOF for ultraselective and fast mercury confinement (Figs. 1 and S5). The affinity binding being ensured by resemblance, similarly to what is observed for the mercury reductase (MR) enzyme (Scheme S2),[56] whilst selectivity and kinetics fine controlled by size and shape of the pores. Such size selectivity also precludes the adsorption of other possible water contaminants of bigger size, i.e. organic dyes.

In spite of the same nature of the ligand employed to construct **1** and a high performing MOF for mercury removal, previously reported by us,[42] it is stimulating to note that methionine residue behaves differently. It can be either flexible in bigger pores,[42] enhancing levels of loading, or more rigid in smaller pores and thus modest in loading but more selective and faster when capturing $HgCl_2$ molecules in **1**. These results indicate how a meticulous choice of the ligand together with a fine tuning of synthetic subtle factors, not only related to pore's dimensions, must be taken into account to design and synthesised porous materials.

The experimental powder X-ray diffraction (PXRD) patterns of polycrystalline samples **1**, **0.5HgCl$_2$@1** and **HgCl$_2$@1** are consistent with the theoretical patterns (Fig. 2a). This confirms the purity of the samples as well as the isostructurality of the bulk with the crystals selected for single crystal X-ray diffraction. The water contents were established by TGA (Fig. S10).

ICP and SEM/EDX analyses, combined with single crystal X-ray diffraction, confirmed that compound **1** is capable to capture $HgCl_2$ from aqueous solution as other MOFs[38–44,57] and COFs,[33,58,59] through the abovementioned dual step capture process to give **0.5HgCl$_2$@1** and **HgCl$_2$@1**. The $HgCl_2$ loading, even in the case of **HgCl$_2$@1** (*ca.* 28.6 wt. %), is relatively modest compared to those of some of the mentioned recent works. This is related to the small size of the pores in **1**. Nevertheless, for successful application of **1** in water cleaning,

View Article Online
DOI: 10.1039/C7TA06199D

other factors such as selectivity, kinetics and, especially, the ability to reduce drastically mercury concentration, are more important than the total sorption capacity. In this respect, the great stability conferred by such functional confined space to the resulting $HgCl_2S_2$ species, as revealed by the crystal structure, make this material an ideal candidate to perform efficiently the selective capture of $HgCl_2$ from water.

Firstly, aiming at analysing the selectivity of the capture process, 100 mg of a polycrystalline sample of **1** were dispersed in an aqueous solution of $HgCl_2$ (2 mmol) containing also the same quantity of other metal cations regularly present in water for human consumption, such as NaCl, $MgCl_2$, $CaCl_2$, $AlCl_3$ and $FeCl_3$ (see ESI†). The metal adsorption process was monitored, through ICP-MS analysis of the increase of the metal salts within the MOF at specific time intervals (Fig. 2b and Table S3, ESI†). These analyses indicated that only the mercury salt is adsorbed by **1**, showing a great selectivity, due to the high affinity of the sulphur atoms for mercury. Moreover, Fig. 2b confirms the extremely fast kinetic profile for the $HgCl_2$ capture (Fig. S1 and Table S2), even in the presence of the other metal ions. ICP-MS also confirmed that no Cu^{2+} leeching occurs during the process.

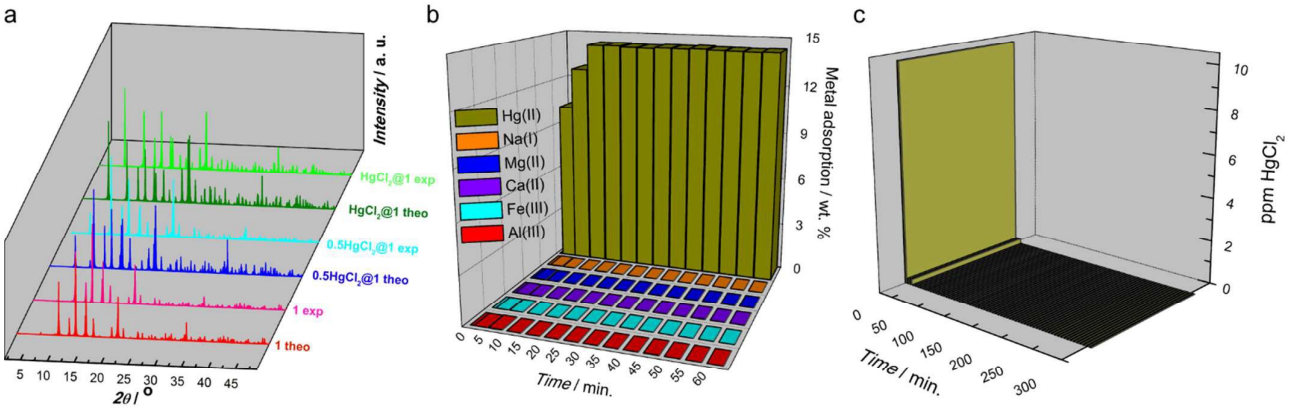

Fig. 2. a. Calculated and experimental PXRD pattern profiles of **1**, **0.5HgCl$_2$@1** and **HgCl$_2$@1** (see legend), in the 2ϑ range 2–50°. **b**. Hg^{II} (gold), Na^{I} (orange), Mg^{II} (blue), Ca^{II} (purple), Fe^{III} (cyan) and Al^{III} (red) adsorption *vs.* time curves of by **1** in a equimolar metal solution. **c**. Decrease of [$HgCl_2$] with time (gold) after soaking 50 mg of **1** in a 10 ppm $HgCl_2$ aqueous solution in the 0-300 min. interval.

The efficiency of **1** in cleaning contaminated waters is shown in Fig. 2c. 50 mg of a polycrystalline sample of **1** were soaked, under soft stirring, in a 10 ppm aqueous solution of $HgCl_2$. The removal efficiency was followed through the decrease of the concentration of the mercury salt (Fig. 2c and Table S4) at specific time intervals (0-1440 min) of immersion of **1** in the solution. Fig. 2c shows an extremely efficient and fast process. After only five minutes, **1** has captured already the 99.7% of the $HgCl_2$ and, ten minutes later, [$HgCl_2$] has decreased below 2 ppb, within permissible limits in drinking water.[60] Overall, these results situate compound **1** within the best performing materials, and the best among MOFs, in mercury removal. Only very few reported compounds are capable to reduce [$HgCl_2$] so fast and drastically (Fig. 3). The closer to the lower left corner of the diagram, the better the performance of the material. The reasons for this particularly good behaviour have to be found in the stable conformation adopted by the mercury centre, which is similar to the conformation of the MR, as previously observed,[42] in combination with the appropriate confined space provided by the pore. This strategy somehow moves in a different direction than that of other porous systems with larger channels, which enable higher loadings but, sometimes, lower capture efficiencies.

Finally, we verified that **1** can be reused and thus, that the capture process is reversible. In this respect, $HgCl_2$ was extracted after suspension of **0.5HgCl$_2$@1** in 2-mercaptoethanol for 24 hours. ICP-MS confirmed that all $HgCl_2$ was extracted after this short period of time and the crystallinity of the material after the extraction process (**1'**) was confirmed by its PXRD pattern (Fig. S11).

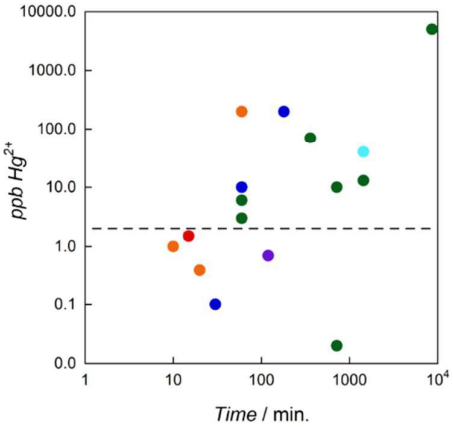

Fig. 3. Comparison of the decrease of [Hg^{2+}] in contaminated aqueous solutions and the time required to achieve such decrease for **1** (red), and different materials reported such as MOFs[38–44] (green), COFs[33,58,59] (covalent-organic frameworks, blue), POPs[31,32,61] (porous organic polymers, orange), mesoporous silicas[62] (purple) and chalcogels[63] (cyan). Dashed line represent the frontier between contaminated and accepted limits for drinking water.[60]

View Article Online
DOI: 10.1039/C7TA06199D

Additionally to the metal capture experiments, and aiming at further exploring the potential of our approach, we carried out gas adsorption measurements. The N_2 (77 K, 298 K), CO_2 (273 K, 298 K) isotherms indicate that only CO_2 is adsorbed significantly (Fig. S12). The differences in the kinetic diameters of these molecules are very small, namely a kinetic diameter of CO_2 of *ca.* 0.33 nm and *ca.* 0.36 nm for N_2, while compound **1** shows a pore aperture situated in this narrow range. On the basis of these results, breakthrough experiments were carried out at 298 K and 1 bar for binary mixtures of different gases whose kinetic diameters range between 0.33 and 0.37 nm (ca. 0.33 for CO_2, 0.36 for N_2, 0.37 for CH_4,). Thus, CH_4/CO_2 (75/25) and N_2/CO_2 (75/25) were separated using packed columns (*ca.* 1 g) of **1** (Fig. S13) as stationary phases. Before breakthrough of CO_2, **1** shows almost infinite selectivities for the separation of CH_4/CO_2 and N_2/CO_2 gas mixtures. The complete sorption of CO_2 confirms that the pores are large enough to allow very fast kinetics. The much faster breakthrough of N_2 and CH_4 is in agreement with their lower sorption capacity. This opens perspectives for further studies aimed at limiting the pore window in MOFs as a strategy to achieve effective gas separations in for instance Mixed Matrix Membranes, where MOFs are dispersed in a polymer matrix.[64]

Conclusions

In summary, we report a new water-stable and eco-friendly MOF featuring very small square functional channels, capable to capture hazardous species such as $HgCl_2$ from aqueous media. The specific positions occupied by the thioalkyl groups decorating the pores of the MOF, together with the strong affinity of S atoms for mercury, and the confined state provided by the MOF pores, enables strong and specific coordinative interactions and contributes to the very stable tetrahedral conformation of the resulting $HgCl_2S_2$ adduct. These structural features account for the very selective and efficient capture process. Indeed, compound **1** is capable to purify contaminated water better than most materials reported so far, reducing the [$HgCl_2$] to below 2 ppb, within the maximum limits for drinking water. In addition, despite the narrow pore sizes, the diffusion is not negatively affected and the capture process is extremely fast (less than 15 minutes to capture more than 99.95% of the $HgCl_2$). Finally, **1** can be environmentally friendly and easily synthesised in large amounts with low cost, offering realistic possibilities for commercialization and practical application. The development of highly selective MOFs with lower overall capacity may offer a more successful approach for the development of selective heavy metal removal adsorbents, than the development of novel MOFs with lower selectivity and efficiency but higher overall capacity. This novel material situates among the fastest and more efficient materials cleaning up mercury contaminated waters (Fig. 3). Finally, very strong difference in gas sorption by these MOFs makes them potentially useful in a wider range of application fields, such as gas separation membranes.

Acknowledgements

This work was supported by the MINECO (Spain) (Project CTQ2016-75671-P and Excellence Unit "Maria de Maeztu" MDM-2015-0538), the Generalitat Valenciana (Spain) (Project PROMETEOII/2014/070) and the Ministero dell'Istruzione, dell'Università e della Ricerca (Italy). M. M. and X. Q. thank the MINECO and the China Scholarship Council for grants. Thanks are also extended to the Ramón y Cajal program (E.P and E. V. R.-F.). We also acknowledge SOLEIL and DIAMOND for provision of synchrotron radiation facilities and thank Dr. Pierre Fertey and Dr. David Allan for their assistance.

Notes and references

1 S. Kitagawa and R. Matsuda, *Coord. Chem. Rev.*, 2007, **251**, 2490–2509.
2 G. Férey, *Chem. Soc. Rev.*, 2008, **37**, 191–214.
3 J. R. Long and O. M. Yaghi, *Chem. Soc. Rev.*, 2009, **38**, 1213–4.
4 O. K. Farha and J. T. Hupp, *Acc. Chem. Res.*, 2010, **43**, 1166–1175.
5 H. Furukawa, K. E. Cordova, M. O'Keeffe and O. M. Yaghi, *Science*, 2013, **341**, 974.
6 Y. Cui, B. Li, H. He, W. Zhou, B. Chen and G. Qian, *Acc. Chem. Res.*, 2016, **49**, 483–493.
7 J. Li, J. Sculley and H. Zhou, *Chem. Rev.*, 2012, **112**, 869–932.
8 J. Ferrando-Soria, P. Serra-Crespo, M. de Lange, J. Gascon, F. Kapteijn, M. Julve, J. Cano, F. Lloret, J. Pasán, C. Ruiz-Pérez, Y. Journaux and E. Pardo, *J. Am. Chem. Soc.*, 2012, **134**, 15301–4.
9 Q. Li, W. Zhang, O. S. Miljanic, C.-H. Sue, Y.-L. Zhao, L. Liu, C. B. Knobler, J. F. Stoddart and O. M. Yaghi, *Science*, 2009, **325**, 855–859.
10 Y. Inokuma, T. Arai and M. Fujita, *Nat. Chem.*, 2010, **2**, 780–783.
11 R. Matsuda, *Nature*, 2014, **509**, 434–435.
12 V. Duplan, M. Hoshino, W. Li, T. Honda and M. Fujita, *Angew. Chemie Int. Ed.*, 2016, **55**, 4919–4923.
13 A. Abhervé, T. Grancha, J. Ferrando-Soria, M. Clemente-León, E. Coronado, J. C. Waerenborgh, F. Lloret and E. Pardo, *Chem. Commun.*, 2016, **52**, 7360–7363.
14 M. Mon, A. Pascual-Álvarez, T. Grancha, J. Cano, J. Ferrando-Soria, F. Lloret, J. Gascon, J. Pasán, D. Armentano and E. Pardo, *Chem. Eur. J.*, 2016, **22**, 539–545.
15 P. Li, J. A. Modica, A. J. Howarth, E. Vargas L., P. Z. Moghadam, R. Q. Snurr, M. Mrksich, J. T. Hupp and O. K. Farha, *Chem*, 2016, **1**, 154–169.
16 F. R. Fortea-Pérez, M. Mon, J. Ferrando-Soria, M. Boronat, A. Leyva-Pérez, A. Corma, J. M. Herrera, D. Osadchii, J. Gascon, D. Armentano and E. Pardo, *Nat. Mater.*, 2017, **16**, 760–766.
17 F. M. Tabellion, S. R. Seidel, A. M. Arif and P. J. Stang, *J. Am. Chem. Soc.*, 2001, **123**, 7740–7741.
18 S. M. Cohen, *J. Am. Chem. Soc.*, 2017, **139**, 2855–2863.
19 T. Grancha, J. Ferrando-Soria, H.-C. Zhou, J. Gascon, B. Seoane, J. Pasán, O. Fabelo, M. Julve and E. Pardo, *Angew. Chemie Int. Ed.*, 2015, **54**, 6521–6525.
20 G. A. Olah and Á. Molnár, *Hydrocarbon Chemistry*, John Wiley & Sons, Inc., Hoboken, NJ, USA, 2003.
21 M. Beckner and A. Dailly, *Appl. Energy*, 2015, **149**, 69–74.
22 H. Wu, Q. Gong, D. H. Olson and J. Li, *Chem. Rev.*, 2012, **112**, 836–868.
23 Y. Inokuma, T. Arai and M. Fujita, *Nat. Chem.*, 2010, **2**, 780–783.
24 Y. Inokuma, M. Kawano and M. Fujita, *Nat. Chem.*, 2011, **3**, 349–358.

View Article Online
DOI: 10.1039/C7TA06199D

25 J. Huang, H.-D. Choi, M. S. Landis and T. M. Holsen, *J. Environ. Monit.*, 2012, **14**, 2976.
26 M. J. Griffin, K. M. M. Kabir, V. E. Coyle, A. E. Kandjani, Y. M. Sabri, S. J. Ippolito and S. K. Bhargava, *Environ. Sci. Technol.*, 2016, **50**, 1384–1392.
27 M. Enrico, G. Le Roux, N. Marusczak, L.-E. Heimbürger, A. Claustres, X. Fu, R. Sun and J. E. Sonke, *Environ. Sci. Technol.*, 2016, **50**, 2405–2412.
28 F. De Simone, C. N. Gencarelli, I. M. Hedgecock and N. Pirrone, *Environ. Sci. Technol.*, 2016, **50**, 5154–5162.
29 M. Sadiq, *Toxic Metal Chemistry in Marine Environments*, Marcel Dekker, 1992.
30 Y. Lin, Y. Yang, Y. Li, L. Yang, X. Hou, X. Feng and C. Zheng, *Environ. Sci. Technol.*, 2016, **50**, 2468–2476.
31 N. Dave, M. Y. Chan, P.-J. J. Huang, B. D. Smith and J. Liu, *J. Am. Chem. Soc.*, 2010, **132**, 12668–12673.
32 B. Li, Y. Zhang, D. Ma, Z. Shi and S. Ma, *Nat. Commun.*, 2014, **5**, 5537.
33 S.-Y. Ding, M. Dong, Y.-W. Wang, Y.-T. Chen, H.-Z. Wang, C.-Y. Su and W. Wang, *J. Am. Chem. Soc.*, 2016, **138**, 3031–3037.
34 S. Kabiri, D. N. H. Tran, M. A. Cole and D. Losic, *Environ. Sci. Water Res. Technol.*, 2016, **2**, 390–402.
35 M. Banerjee, R. Karri, K. S. Rawat, K. Muthuvel, B. Pathak and G. Roy, *Angew. Chemie Int. Ed.*, 2015, **54**, 9323–9327.
36 Y. Oh, C. D. Morris and M. G. Kanatzidis, *J. Am. Chem. Soc.*, 2012, **134**, 14604–14608.
37 K. S. Subrahmanyam, C. D. Malliakas, D. Sarma, G. S. Armatas, J. Wu and M. G. Kanatzidis, *J. Am. Chem. Soc.*, 2015, **137**, 13943–13948.
38 J. He, K.-K. Yee, Z. Xu, M. Zeller, A. D. Hunter, S. S.-Y. Chui and C.-M. Che, *Chem. Mater.*, 2011, **23**, 2940–2947.
39 K.-K. Yee, N. Reimer, J. Liu, S.-Y. Cheng, S.-M. Yiu, J. Weber, N. Stock and Z. Xu, *J. Am. Chem. Soc.*, 2013, **135**, 7795–7798.
40 T. Liu, J.-X. Che, Y.-Z. Hu, X.-W. Dong, X.-Y. Liu and C.-M. Che, *Chem. Eur. J.*, 2014, **20**, 14090–14095.
41 F. Luo, J. L. Chen, L. L. Dang, W. N. Zhou, H. L. Lin, J. Q. Li, S. J. Liu and M. B. Luo, *J. Mater. Chem. A*, 2015, **3**, 9616–9620.
42 M. Mon, F. Lloret, J. Ferrando-Soria, C. Martí-Gastaldo, D. Armentano and E. Pardo, *Angew. Chemie Int. Ed.*, 2016, **55**, 11167–11172.
43 L. Liang, Q. Chen, F. Jiang, D. Yuan, J. Qian, G. Lv, H. Xue, L. Liu, H.-L. Jiang and M. Hong, *J. Mater. Chem. A*, 2016, **4**, 15370–15374.
44 A. Chakraborty, S. Bhattacharyya, A. Hazra, A. C. Ghosh and T. K. Maji, *Chem. Commun.*, 2016, **52**, 2831–2834.
45 A. C. McKinlay, R. E. Morris, P. Horcajada, G. Férey, R. Gref, P. Couvreur and C. Serre, *Angew. Chemie Int. Ed.*, 2016, 2010, 49, 6260–6266.
46 I. Imaz, M. Rubio-Martínez, J. An, I. Solé-Font, N. L. Rosi and D. Maspoch, *Chem. Commun.*, 2011, **47**, 7287–7302.
47 T. Grancha, J. Ferrando-Soria, J. Cano, P. Amorós, B. Seoane, J. Gascon, M. Bazaga-García, E. R. Losilla, A. Cabeza, D. Armentano and E. Pardo, *Chem. Mater.*, 2016, **28**, 4608–4615.
48 M. Mon, J. Ferrando-Soria, T. Grancha, F. R. Fortea-Pérez, J. Gascon, A. Leyva-Pérez, D. Armentano and E. Pardo, *J. Am. Chem. Soc.*, 2016, **138**, 7864–7867.
49 S. T. Hyde, M. O'Keeffe and D. M. Proserpio, *Angew. Chemie Int. Ed.*, 2008, **47**, 7996–8000.
50 M. O'Keeffe, M. A. Peskov, S. J. Ramsden and O. M. Yaghi, *Acc. Chem. Res.*, 2008, **41**, 1782–1789.
51 A. Lapprand, A. Bonnot, M. Knorr, Y. Rousselin, M. M. Kubicki, D. Fortin and P. D. Harvey, *Chem. Commun.*, 2013, **49**, 8848.
52 T.-T. Luo, L.-Y. Hsu, C.-C. Su, C.-H. Ueng, T.-C. Tsai and K.-L. Lu, *Inorg. Chem.*, 2007, **46**, 1532–1534.
53 E. M. Nolan and S. J. Lippard, *J. Am. Chem. Soc.*, 2007, **129**, 5910–5918.
54 T. Aridomi, K. Takamura, A. Igashira-Kamiyama, T. Kawamoto and T. Konno, *Chem. Eur. J.*, 2008, **14**, 7752–7755.
55 S. Park, S. Y. Lee and S. S. Lee, *Inorg. Chem.*, 2010, **49**, 1238–1244.
56 P. Lian, H.-B. Guo, D. Riccardi, A. Dong, J. M. Parks, Q. Xu, E. F. Pai, S. M. Miller, D.-Q. Wei, J. C. Smith and H. Guo, *Biochemistry*, 2014, **53**, 7211–7222.
57 K.-K. Yee, Y.-L. Wong, M. Zha, R. Y. Adhikari, M. T. Tuominen, J. He and Z. Xu, *Chem. Commun.*, 2015, **51**, 10941–10944.
58 N. Huang, L. Zhai, H. Xu and D. Jiang, *J. Am. Chem. Soc.*, 2017, **139**, 2428–2434.
59 Q. Sun, B. Aguila, J. Perman, L. D. Earl, C. W. Abney, Y. Cheng, H. Wei, N. Nguyen, L. Wojtas and S. Ma, *J. Am. Chem. Soc.*, 2017, **139**, 2786–2793.
60 World Health Organisation, *Guidelines for Drinking-water Quality, Fourth Edition*, 2011.
61 B. Aguila, Q. Sun, J. A. Perman, L. D. Earl, C. W. Abney, R. Elzein, R. Schlaf and S. Ma, *Adv. Mater.*, 2017, **1700665**, 1700665.
62 X. Feng, G. E. Fryxell, L.-Q. Wang, A. Y. Kim, J. Liu and K. M. Kemner, *Science*, 1997, **276**, 923–926.
63 S. Bag, P. N. Trikalitis, P. J. Chupas, G. S. Armatas and M. G. Kanatzidis, *Science,* 2007, **317**, 490–493.
64 H. Vinh-Thang and S. Kaliaguine, *Chem. Rev.*, 2013, **113**, 4980–5028.

View Article Online
DOI: 10.1039/C7TA06199D

Graphical Abstract for the manuscript:

Fine-tuning of the confined space in microporous metal-organic frameworks for efficient mercury removal

Marta Mon, Xiaoni Qu, Jesús Ferrando-Soria,* Isaac Pellicer-Carreño, Antonio Sepúlveda-Escribano, Enrique V. Ramos-Fernandez, Johannes C. Jansen, Donatella Armentano* and Emilio Pardo*

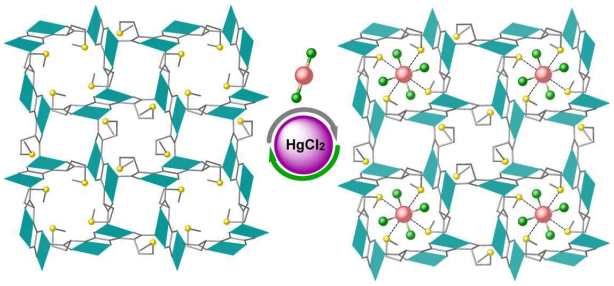

We report a novel metal-organic framework showing a very efficient, selective and fast Hg^{2+} removal.